Synthesis and Evaluation of Some Sulfonamide-Substituted of 1,3,5-Triphenyl Pyrazoline Derivatives as Tyrosinase Enzyme Inhibitors

Noval Herfindo[1], Neni Frimayanti[1]*, Ihsan Ikhtiarudin[1], Yum Eryanti[2], Adel Zamri[2]

[1]Department of Pharmacy, Sekolah Tinggi Ilmu Farmasi Riau, Pekanbaru 28293, Riau, Indonesia
[2]Department of Chemistry, University of Riau, Pekanbaru-28293, Riau, Indonesia

*Corresponding author email : nenifrimayanti@gmail.com

ABSTRACT

Pyrazoline is well-known as heterocyclic compound that can exhibit many biological effects. In this work, we synthesized a series of sulfonamide-substituted 1,3,5-triphenyl pyrazoline compounds as a promising tyrosinase inhibitor agent. These compounds prepared by multicomponent reaction of corresponding aldehyde, ketone, and hydrazine using sealed-vessel reactor. Pyrazoline compounds were tested for their tyrosinase inhibitor activity through *in vitro* assay. The test result found that compounds **4c, 4d,** and **4e** possessed better tyrosinase inhibitory activity compared to the reference inhibitor kojic acid. Compound **4c** exhibited the strongest tyrosinase inhibitory effect with an IC_{50} value of $30.14\,\mu$M. The results suggested that hydroxyl and methoxy substituents at *para* position are preferable. Furthermore, molecular docking studies result match the pattern of *in vitro* assay where the compound will provide a stronger binding interaction and lower binding free energies.

Keywords: Docking, hyperpigmentation, melanin, pyrazoline, sulfonamide, tyrosinase

INTRODUCTION

Tyrosinase enzyme is a copper-containing oxidase which acts as a limiting enzyme in the synthesis of pigments such as melanin and polyphenol compounds (Di Petrillo et al., 2016) Melanin is a pigment that is responsible for the skin, hair and eyes color of humans and animals, which plays a key function in UV protection and is an essential defensive mechanism of the skin against any harmful factors (Pillaiyar et al., 2017; Qin et al. 2015). However, in human the overproduction of melanin in the skin due to tyrosinase overexpression can cause hyperpigmentation consequences such as freckles, melasma, age spots, and melanoma (Cui et al., 2018) Furthermore, tyrosinase also catalyzes the neuromelanin biosynthesis pathway, in which dopamine is oxidized to form dopaquinones. Excessive production of dopaquinones, on the other hand, causes neuronal damage and cell death. This showed that tyrosinase may be involved in the formation of neuromelanin in the human brain, as well as the neurodegeneration associated with Parkinson's and Huntington's disorders (Hasegawa, 2010; Pillaiyar et al., 2017). In terms of agriculture, overproduction of tyrosinase has been associated to the browning of a variety of fruits and vegetables, as well as alterations in their flavor and nutritional value, all of which can reduce their economic worth (Loizzo et al., 2012). Since tyrosinase is the limiting step enzyme in melanogenesis, tyrosinase inhibitors have become essential as depigmenting treatments in hyperpigmentation diseases.

Numerous synthetic tyrosinase inhibitors have been reported, including hydroquinone and kojic acid, which is frequently used in cosmetics to lighten the skin (Chang, 2009). However, there have been some major adverse effects linked to the usage of this chemical. Kojic acid has been linked to contact dermatitis and photosensitivity, while hydroquinone has been linked to exogenous ochronotic, contact dermatitis, corneal melanosis, nail hyperpigmentation, conjunctival hyperpigmentation as well as severe side effects includes peripheral neuropathy, fish odor syndrome, fetal growth retardation (Pollock et al., 2020). Therefore, further studies need to be done to find novel and biocompatible tyrosinase inhibitors that may be employed in the cosmetic and food sectors as whitening and anti-browning agents. Synthesized compounds such as aurones, chalcones, flavanones, and pyrazole derivatives have gotten a lot of interest as tyrosinase inhibitors. Specifically, pyrazoline derivatives because of its ability to interact with the hydrophobic protein pocket around the binuclear copper active site of tyrosinase (Qin et al., 2015).

Pyrazoline are mono-unsaturated 5-membered heterocyclic compounds containing three carbon atoms and two adjacent nitrogen within the ring. This

compound has been reported to have many biological effects such as anticancer, antidiabetic, antidengue virus, antituberculosis (Ahmad et al., 2016; Herfindo et al., 2020; Jasril et al., 2019; Zamri et al., 2019) and pyrazolines with sulfonamide group also exhibit biological activity as urease inhibitor, which makes this compound interesting (Mojzych et al., 2017). Additionally, sulfonamides are a valuable therapeutic class. It exhibits antibacterial, hypoglycemic, high-ceiling diuretic, antithyroid, antiglaucoma properties, and anti-inflammatory (Mojzych et al., 2014). Moreover, a variety of sulfonamides have been reported to act as tyrosinase inhibitor (Lolak et al., 2020; Mojzych et al., 2014; Rahayu et al., 2022). Based on these findings, we explored the tyrosinase enzyme inhibitory activity of sulfonamide-substituted of 1,3,5-triphenyl pyrazoline. The hydroxyl group was also introduced to mimics kojic acid. Then the biological activity of the compounds was compared by molecular docking study and *in vitro* assay to tyrosinase enzyme.

EXPERIMENITAL SECTION
Material and Methods

Starting materials used in this study were purchased from Sigma-Aldrich (purity ≥ 95%) and used without further purification. Reagents used in this study includes 2'-hydroxyacetophenone, 3'-hydroxy acetophenone, 4'-hydroxyacetophenone, 2-methoxy benzaldehyde, 3-methoxybenzaldehyde, 4-methoxy benzaldehyde, 4-hydroxy-3-methoxybenzal dehyde, and 4-hydrazinylbenzene sulfonamide. Organic solvents such as *n*-hexane, ethyl acetate, and methanol obtained from Merck. Fisher-John apparatus (Fisher Scientific, Waltham, MA, USA) (uncorr) was used to determine the melting points. Genesys™ 10S UV–visible spectrophotometer (Thermo Scientific™, Waltham, MA, USA) was used to measure UV absorbance. Shimadzu® FT-IR Prestige-21 spectrophotometer (Shimadzu Corporation, Kyoto, Japan) was used to measure IR spectra in KBr. Agilent® (Agilent Technologies, Santa Clara, CA, USA) was used to measure the proton and carbon NMR spectra with trimethylchlorosilane (TMS) as internal standard and deuterated chloroform (CDCl$_3$ as solvent). Water Xevo QTOFMS instrument (Waters, Milford, MA, USA) was used to measure atomic mass of synthesized compound.

Synthesis of 4-Hydrazinylbenzenesulfonamide (3)

Compounds **3** as one of starting material for this study was prepared according to previously reported literature (Rahayu et al., 2022).

General Synthesis Procedure of Pyrazolines (4a-f)

Each pyrazoline compound, C$_{22}$H$_{21}$N$_3$O$_4$S (4a-c, 4e-f) and C$_{22}$H$_{21}$N$_3$O$_5$S (4d) was synthesized by reacting various hydroxylated acetophenone **1** (1 mmol), substituted benzaldehyde **2** (1 mmol), and 4-hydrazinylbenzenesulfonamide **3** (2 mmol) with the presence of sodium hydroxide solution (30%, 1mL) in

absolute ethanol (5 mL). The reaction was performed in a pressure tube with a stir bar using sealed-vessel reactor (Monowave 50) at 80 ℃ for 2 hours. After the completion of reaction, the mixture was poured to crushed ice to yield solid product. The solid crude product was filtered, washed, and then recrystallized using methanol to yield pyrazolines **4a-f.**

4-(3-(2-hydroxyphenyl)-5-(4-methoxyphenyl)-4,5-dihydro-1H-pyrazol-1-yl)benzene sulfonamide **(4a)** as white solid with 27 % yield. Melting point 212-213 °C. UV (EtOH): λ$_{max}$ = 362 nm. FTIR (KBr) ū (cm^{-1}): 3386, 3318, 3273, 3017, 2970, 1594, 1513, 1330, 1248, 1150. ^{1}H NMR (500 MHz, DMSO-d$_6$) δ (ppm): δ 9.84 (s, 1H, OH), 7.60 (d, *J* = 8.5 Hz, 2H, ArH), 7.51 (d, *J* =8.0 Hz, 1H, ArH), 7.30 (t, *J* = 8,3 Hz, 1H, ArH), 7.19 (d, *J* = 8.2 Hz, 2H, ArH), 7.04 (s, 2H, NH$_2$), 7.01 (d, *J* = 8.5 Hz, 2H, ArH), 6.98 (d, *J* = 8.2 Hz, 1H, ArH), 6.93 (t, *J* = 7.8 Hz, 1H, ArH), 6.89 (d, *J* = 8.3 Hz, 2H, ArH), 5.56 (dd, *J* = 12.0, 5.3 Hz, 1H, Hx), 4.05 (dd, *J* = 18.0, 12.0 Hz, 1H, H$_B$), 3.70 (s, 3H, OCH$_3$), 3.29 (dd, *J* = 18.0, 5.3 Hz, 1H, H$_A$). HRMS (m/z): [M+H]$^+$ found 424.1328 (calculated mass for C$_{22}$H$_{21}$N$_3$O$_4$S is 424.1331).

4-(3-(3-hydroxyphenyl)-5-(4-methoxyphenyl)-4,5-dihydro-1H-pyrazol-1-yl)benzene sulfonamide **(4b)** as yellow solid with 63 % yield. Melting point 190-192 °C. UV (EtOH): λ$_{max}$ = 358 nm. FTIR (KBr) ū (cm^{-1}): 3610, 3363, 3271, 3070, 2900, 1591, 1512, 1335, 1247, 1153. ^{1}H NMR (500 MHz, DMSO-d$_6$) δ (ppm): δ 9.60 (s, 1H, OH), 7.58 (d, *J* = 8.6 Hz, 2H, ArH), 7.24 (t, *J* = 8.2 Hz, 1H, ArH), 7.23-7.24 (m, 1H, ArH), 7.17 (s, 1H, ArH), 7.16 (d, *J* = 8.7 Hz, 2H, ArH), 7.05 (d, *J* = 8.6 Hz, 2H, ArH), 7.01 (s, 2H, NH$_2$), 6.88 (d, *J* = 8.7 Hz, 2H, ArH), 6.81 (d, *J* = 8.2 Hz, 1H, ArH), 5.55 (dd, *J* = 12.0, 5.1 Hz, 1H, Hx), 3.89 (dd, *J* = 17.6, 12.0 Hz, 1H, H$_B$), 3.69 (s, 3H, OCH$_3$), 3.08 (dd, *J* = 17.6, 5.1 Hz, 1H, H$_A$). HRMS (m/z): [M+H]$^+$ found 424.1352 (calculated mass for C$_{22}$H$_{21}$N$_3$O$_4$S is 424.1331).

4-(3-(4-hydroxyphenyl)-5-(4-methoxyphenyl)-4,5-dihydro-1H-pyrazol-1-yl)benzene sulfonamide **(4c)** as yellow solid with 71 % yield. Melting point 152-154 °C. UV (EtOH): λ$_{max}$ = 357 nm. FTIR (KBr) ū (cm^{-1}): 3365, 3247, 3009, 2957, 1592, 1507, 1330, 1245, 1150. ^{1}H NMR (500 MHz, DMSO-d$_6$) δ (ppm): δ 9.87 (s, 1H, OH), 7.62 (d, *J* = 8.6 Hz, 2H, ArH), 7.55 (d, *J* = 8.6 Hz, 2H, ArH), 7.15 (d, *J* = 8.6 Hz, 2H, ArH), 7.02 (d, *J* = 8.6 Hz, 2H, ArH), 6.98 (s, 2H, NH$_2$), 6.88 (d, *J* = 8.6 Hz, 2H, ArH), 6.83 (d, *J* = 8.6 Hz, 2H, ArH), 5.49 (dd, *J* = 11.9, 4.9 Hz, 1H, Hx), 3.86 (dd, *J* = 17.5, 11.9 Hz, 1H, H$_B$), 3.69 (s, 3H, OCH$_3$), 3.08 (dd, *J* = 17.5, 4.9 Hz, 1H, H$_A$). HRMS (m/z): [M+H]$^+$ found 424.1326 (calculated mass for C$_{22}$H$_{21}$N$_3$O$_4$S is 424.1331).

4-(3-(4-hydroxyphenyl)-5-(4-hydroxy-3-methoxyphenyl)-4,5-dihydro-1H-pyrazol-1-yl)benzene sulfonamide **(4d)** as yellow solid with 25 % yield. Melting point 198-200 °C. UV (EtOH): λ$_{max}$ = 351 nm. FTIR (KBr) ū (cm^{-1}): 3324, 3286, 3211, 3026, 2970,

1601, 1516, 1320, 1238, 1155. ^{1}H NMR (500 MHz, DMSO-d_6) δ (ppm): δ 10.56 (s, 1H, OH), 9.86 (s, 1H, OH), 7.67-7.59 (m, 8H, ArH), 7.55 (d, J = 8,7 Hz, 2H, ArH), 7.09 (d, J = 8.6 Hz, 2H, ArH), 6.98 (s, 2H, NH$_2$), 6.86 (d, J = 2,1 Hz, 1H, ArH), 6.68 (d, J = 8.1 Hz, 1H, ArH), 6.56 (dd, J = 8.1, 2.0 Hz, 1H, ArH), 5.40 (dd, J = 11.9, 5.4 Hz, 1H, H$_X$), 3.85 (dd, J = 17.4, 11.9 Hz, 1H, H$_B$), 3.83 (s, 3H, OCH$_3$), 3.10 (dd, J = 17.4, 5.4 Hz, 1H, H$_A$). HRMS (m/z): [M+H]$^+$ found 440.1269 (calculated mass for C$_{22}$H$_{22}$N$_3$O$_5$S is 440.1280).

4-(3-(4-hydroxyphenyl)-5-(3-methoxyphenyl)-4,5-dihydro-1H-pyrazol-1-yl)benzene sulfonamide (**4e**) as yellow solid with 27 % yield. Melting point 181-182 °C. UV (EtOH): λ$_{max}$ = 359 nm. FTIR (KBr) ū (cm^{-1}): 3336, 3238, 3052, 2907, 1591, 1502, 1327, 1256, 1152. ^{1}H NMR (500 MHz, DMSO-d_6) δ (ppm):) δ 9.87 (s, 1H, OH), 7.62 (d, J = 8.6 Hz, 2H, ArH), 7.56 (d, J = 8.9 Hz, 1H, ArH), 7.24 (dd, J = 9.1, 7.6 Hz, 1H, ArH), 7.05 – 6.98 (m, 4H, ArH, NH$_2$), 6.85 – 6.79 (m, 4H, ArH), 6.76 (d, J = 7.7 Hz, 1H, ArH), 5.52 (dd, J = 11.9, 5.0 Hz, 1H, H$_X$), 3.89 (dd, J = 17.5, 12.0 Hz, 1H, H$_B$), 3.70 (s, 3H, OCH$_3$), 3.11 (dd, J = 17.5, 5.0 Hz, 1H, H$_A$). HRMS (m/z): [M+H]$^+$ found 424.1333 (calculated mass for C$_{22}$H$_{21}$N$_3$O$_4$S is 424.1331).

4-(3-(4-hydroxyphenyl)-5-(2-methoxyphenyl)-4,5-dihydro-1H-pyrazol-1-yl)benzene sulfonamide (**4f**) as yellow solid with 87 % yield. Melting point 148-150 °C. UV (EtOH): λ$_{max}$ = 342 nm. FTIR (KBr) ū (cm^{-1}): 3367, 3275, 3237, 3075, 2841, 1592, 1507, 1328, 1248, 1156. ^{1}H NMR (500 MHz, DMSO-d_6) δ (ppm): δ 9.88 (s, 1H, OH), 7.60 (d, J = 8.6 Hz, 2H, ArH), 7.56 (d, J = 8.6 Hz, 2H, ArH), 7.24 (m, 1H, ArH), 7.09 (d, J = 8.2 Hz, 1H, ArH), 6.99 (s, 2H, NH$_2$), 6.93 (d, J = 8.6 Hz, 2H, ArH), 6.83-6.78 (m, 4H, ArH), 5.65 (dd, J = 12.4, 4.8 Hz, 1H, H$_X$), 3.91 (s, 3H, OCH$_3$), 3.85 (dd, J = 17.5, 12.4 Hz, 1H$_A$), 3.01 (dd, J = 17.5, 4.8 Hz, 1H$_B$). HRMS (m/z): [M+H]$^+$ found 424.1333 (calculated mass for C$_{22}$H$_{21}$N$_3$O$_4$S is 424,1331).

Molecular Docking Studies

Molecular docking was performed to predict plausible binding mode of synthesized compound in the active site of tyrosinase. In this study, docking was performed using MOE 2020.0901 (Chemical computing group) software package. All synthesized compound structures were sketched using ChemDraw 17 for then these compounds were converted into 3D structure and minimized their energy with the protocol set up MMF94x as selected force field. Protein preparation consisted of some steps, it was begun with download the protein from the protein databank with PDB ID 2Y9X (www.rcsb.org), followed with water removed, alpha carbon and backbone atom minimized. Amino acid residues that have interacted with the native ligand were noted and keep in 2D. Furthermore, chain A was prepared in MOE 2020.0901 using the following steps. It was begun with deleted the ligand followed with selected the

forcefield (CHARMM27). QuickPrep tools in MOE 2020.0901 was used for the protein preparation. Finally, this protein was saved in PDB format for then it was ready used as receptor. Active site of the protein was observed using site finder. Re-docking was performed with the placement and refinement of 50 and 10, respectively. The best spatial arrangement of the re-docked ligand was chosen with RMSD value less than 2 with the same interaction between re-docked ligand and the native ligand.

Mushroom Tyrosinase Enzyme Inhibition Assay

The pyrazoline compounds tyrosinase inhibitory activity were measured using a previously published method with minor adjustments (Cui et al., 2018). The substrates in this test were L-tyrosine. In a 96-well microtiter plate, 40 microliters of L-tyrosine (10 mM) were combined with 80 microliters of phosphate buffer (0.1 M, pH 6.8) and incubated for 10 minutes at 37 °C. Each well on the plate was then filled with 40 microliters of pyrazoline compounds (500, 250, 125, 61.5, 31.125 g/mL in 50% DMSO) and 40 microliters of mushroom tyrosinase (250 U/mL, in PBS), and the absorbance characteristics of the resulting mixtures were measured at 475 nm using a microplate reader. PBS was utilized as a blank control instead of the test sample, and kojic acid (50 μg/mL) was employed as a positive control. For each enzyme assay, the inhibition was calculated as follows:

$$\% \, Inhibition = \frac{ABS_{control} - ABS_{sample}}{ABS_{control}} \times 100$$

Each experiment was performed in triplicate (n=3). The IC$_{50}$ value was measured by using nonlinear regression analysis of the dose-response curves.

RESULTS AND DISCUSSION

Sulfonamide-substituted 1,3,5-triphenyl pyrazoline 4a-f have been obtained from the one-pot reaction between aromatics aldehydes, aromatics ketones, and hydrazine derivate by using a closed-vessel reactor. The synthetic pathway for the desired compounds is depicted in **Figure 1**. In general, pyrazoline formation reactions can be carried out under acidic and basic conditions (Farooq & Ngaini, 2020). In this study, the reaction was carried out in presence of sodium hydroxide which gave good yield. As consequence, pyrazoline is formed through the formation of chalcone as an intermediate, followed by the formation of a pyrazoline ring by a cyclo-condensation reaction with hydrazine.

The compounds of **4a-c** have different in position of hydroxyl group in the aromatic ring. In this case, **4b** and **4c** showed better yields than 4a because the hydroxyl group in *meta* (**4b**) and *para* (**4d**) make them avoid from unwanted intramolecular cyclization. This unwanted reaction can be observed when we used 2'-hydroxyacetophenone as starting material (Zamri et al., 2016). The *ortho* position of hydroxyl group at starting material of **4a** is possible to lead by product

formation and reduce the possibility the reaction between the chalcone intermediate and another starting material (4-hydrazinylbenzenesulfonamide). So that, the compound 4a is obtained in low yield.

In case of compounds **4d-f**, although the hydroxyl groups in acetophenones as their starting materials are in same position (*para*), there are differences in the type and position of substituents of benzaldehydes as their starting materials. The presence of two substituents (4-hydroxy and 3-methoxy) at benzaldehyde as starting material of **4d** suspected of causing steric hindrance that can reduce the yield. Then, compound **4f** with the higher yield than compounds **4c** dan **4e** were caused the presence of methoxy group in *ortho* position of starting material of **4f** that given a bigger impact from negative induction effect, so that the carbonyl group of benzaldehyde as starting material of **4f** become more reactive that the other monomethoxy benzaldehydes (*meta* and *para*). Another researcher has also reported the similar phenomena that the presence of monomethoxy substituent in *ortho* position of the benzaldehyde as starting material is also observed to give higher yield than *meta* and *para* (Dona et al., 2022).

The formation of pyrazoline compounds were confirmed by spectroscopic analyses. The FTIR spectra of **4a-f** show the similarity in absorption pattern. Two absorption bands around ū 3386 and 3275 cm^{-1} show the presence of asymmetrical and symmetrical stretching of the N-H in the sulfonamide (SO_2NH_2) group, while the absorption at the range ū 1591 – 1601 cm^{-1} show the presence of C=N stretch and the absorptions around ū 1335-1320 cm^{-1} indicate the stretching vibration of the C-N bond on the pyrazoline ring. In addition, the absorptions around ū 3075-3017 and ū 1516-1502 cm^{-1} indicate the presence of aromatic rings. Then, the broad absorption bands around ū 3273-3211 cm^{-1} indicate the stretching

vibration of phenolic O-H bond. Furthermore, absorption bands around ū 1256-1238 and ū 1156-1150 cm^{-1} indicate the vibration of the C-O bond from the methoxy substituent and the S=O bond of sulfonamide group, respectively.

^{1}H NMR spectra of compounds **4a-f** emphasize the formation of pyrazoline ring, by the appearance of the ABX protons pattern in the upfield region, as shown in **Figure 2**. In this case, the protons H_A and H_B are in the *geminal* position of the methylene carbon of the pyrazoline ring, while H_X is a proton from the methine carbon of the pyrazoline ring. The peaks of protons H_A appear at range δ_H 3.01 - 3.29 ppm (*dd*, 1H), protons H_B appear at range δ_H 3.85 - 4.05 ppm (*dd*, 1H), and protons H_X appear at range δ_H 5.40 - 5.56 ppm (*dd*, 1H). The difference in chemical shift between the two methylene protons (H_A and H_B) is due to the anisotropic effect of the bonding atom to the chiral carbon atom. Each ABX peak appears as double of doublet (*dd*) with the difference in their coupling constants, where the proton H_A has *geminal* coupling with proton H_B and *vicinal* coupling with proton Hx (J_{AB} = 17.4 - 18.0 Hz and J_{AX} = 4.8 - 5.4 Hz), proton H_B has *geminal* coupling with proton Ha and *vicinal* coupling with proton Hx (J_{BA} = 17.4 - 18.0 Hz and J_{BX} = 11.9 - 12.4 Hz), whereas proton Hx showed the *vicinal* coupling with proton H_A and H_B (J_{XA} = 4.8 - 5.4 Hz and J_{XB} = 11.9 - 12.4 Hz). The ^{1}H NMR spectra also showed a singlet peak of phenolic OH proton at the range δ_H 10.56 – 9.60 ppm (s, 1H), NH_2 protons of sulfonamide at the range δ_H 7.04 - 6.98 ppm (s, 2H), aromatic protons at the range δ_H 7.67 – 6.56 ppm, and methoxy protons at the range δ_H 3.83-3.69 ppm (s, 3H). Overall, the ^{1}H NMR spectra of synthesized pyrazolines has accordance between the number of protons of the obtained compounds and the target molecules. In this case, there are 21 protons in each of pyrazoline compounds.
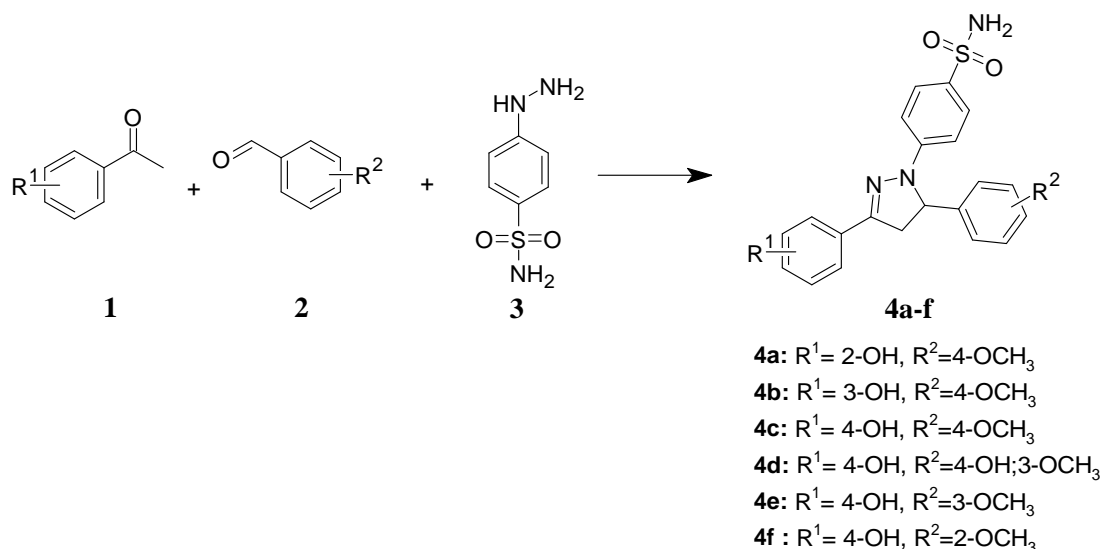

4a: R^1= 2-OH, R^2=4-OCH$_3$
4b: R^1= 3-OH, R^2=4-OCH$_3$
4c: R^1= 4-OH, R^2=4-OCH$_3$
4d: R^1= 4-OH, R^2=4-OH;3-OCH$_3$
4e: R^1= 4-OH, R^2=3-OCH$_3$
4f : R^1= 4-OH, R^2=2-OCH$_3$

Figure 1. Synthesis of 1,3,5-pyrazoline compounds **4a-f** under base condition (NaOH 30%, 1mL) at 80 ºC for 2 hours.
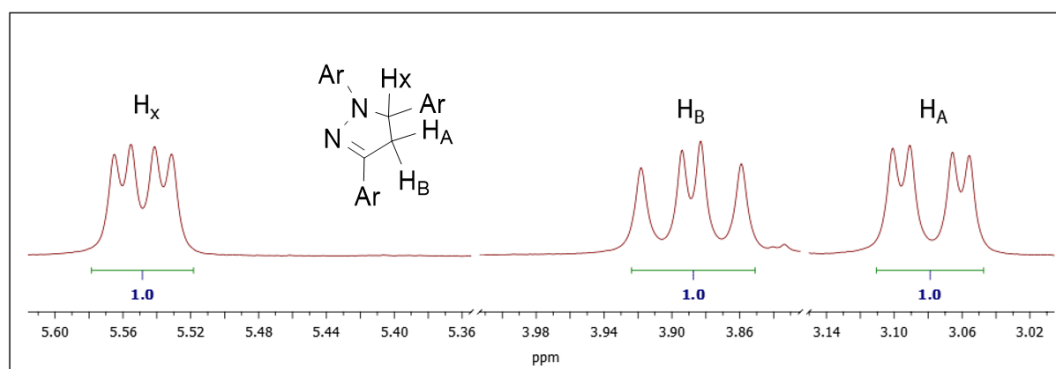
Figure 2. The suggested positions for H_A, H_B, and H_X on the pyrazoline ring and the multiplicities of their ABX peaks in the ^1H NMR spectra of synthesized compounds

Finally, the formations of target molecules were also confirmed through mass spectroscopic data. The molecular weight of each compound was calculated as $[M+H]^+$ and the molecular ion was found at their corresponding mass with high intensity. In addition, there are only a slight difference between calculated and measured masses. The differences are around 0.0002 – 0.0021 m/z unit. Overall, the difference in masses were still less than 0.0030 m/z unit. Thus, they are still acceptable for compound with molecular weight less than 1000.

Tyrosinase Inhibitory Activity

In this work, the biological effect of pyrazoline compounds was evaluated. The monophenolase activity assay was used to test the tyrosinase inhibitory activity of these compounds. The reference drug in this experiment was kojic acid. Kojic acid is a fungus metabolite with inhibitory effect against tyrosinase. The ability of kojic acid to chelate copper at the active site of this enzyme has been attributed to its inhibitory effects in this context (Qin et al., 2015). As a result, kojic acid is frequently utilized as a positive control while searching for novel tyrosinase inhibitors. The effects of compound **4c** on mushroom tyrosinase monophenolase activity were investigated using L-tyrosine as a substrate and kojic acid as a control. Initially, three compounds (**4a-c**) were screened for their inhibitory activity. The results found that **4c** had the significant effect to the enzyme with IC_{50} value of 30.14 μM. Hydroxyl substituent of ring A at *ortho* and *meta* position is not preferable whereas the IC_{50} values of **4a** and **4b** were > 100 μM (Table 1). Furthermore,

4c activity was compared to pyrazoline with different substituent position at ring B (**4d-f**). Similar pattern has been found where the inhibitory activity decreases when the substituent is attached at *ortho* or *meta* position. On other hand, **4d** inhibitory activity is on par with **4c**. It suggests that substituent (-OR and -OH) at *para* position play important role in the activity. In brief, some synthesized sulfonamide-substituted 1,3,5-triphenyl pyrazoline derivate have ability to prevent L-tyrosine from being oxidized. Compound **4c**, **4d** and **4e** have better inhibitory activity compared kojic acid as reference drug and **4c** had the best activity among them.

Molecular Docking

Molecular docking was conducted to predict the binding orientation of pyrazoline with tyrosinase enzyme and also to ensure the *in vitro* results (Jusril et al., 2020). Generally, re-docking of native ligand from the protein (i.e., tyrosinase) was used to validate the selection of docking protocol. In this study, re-docking of native ligand (tropolone) has the binding free energy of -8.1907 kcal/mol with root mean square deviation of 1.4149. RMSD is also play an important role to evaluate the docking accuracy with the value of acceptable range less than 2 (Castro et al., 2017; Makeneni et al., 2018; Yusuf et al., 2008). Furthermore, the validated docking protocols can be used for docking compound **4a-4f**. Pose with the lowest binding free energy was selected as the best docked-pose and the docking results are depicted in **Table 2.**

Table 1. IC_{50} values of synthesized compound

Compound	R^1	R^2	IC_{50} (μM)
4a	2-OH	4-OCH₃	> 100
4b	3-OH	4-OCH₃	> 100
4c	4-OH	4-OCH₃	30.14 ± 1.04
4d	4-OH	4-OH; 3-OCH₃	31.62 ± 1.56
4e	4-OH	3-OCH₃	54.28 ± 3.52
4f	4-OH	2-OCH₃	>100
Kojic acid	-	-	87.36 ± 2.83

Table 2. Interaction of synthesized compound (4a-f) in tyrosinase enzyme active site

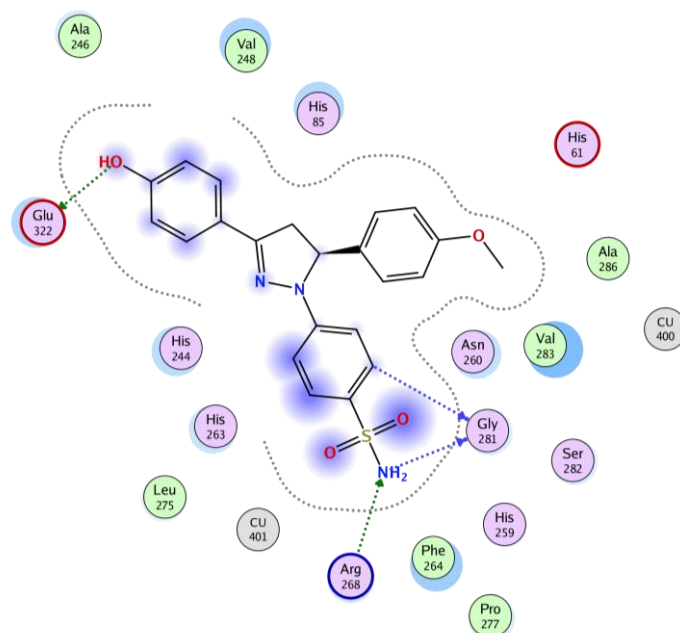| Compound	S (kcal/mol)	RMSD	H bond	Hydro-phobic	van der Walls	The other interactions	Factor of binding
Kojic acid	-4.6302	1.1670	Asn260, Val283	-	His61, Glu256	His85, Glu256, His259, His263, Phe264, Met280, Gly281, Ser282, Ala286, Cu400, Cu401	-
Tropolone	-8,1907	1,4149	-	-	His61, His296	His85, His94, His259, Asn260, His263, Met280, Ser282, Val283, Ala286, Phe292, Cu400, Cu401	9
4a	-8.1525	1.2074	Arg268	-	His61, Glu322	His85, Gly86, His244, Ala246, Val248, His259, Asn260, His263, Phe264, Pro277, Gly281, Ser282, Val283, Ala286, Cu401	10
4b	-8.6994	1.7987	His244, Glu322	Arg268	His61, His296	His85, Gly86, Gly245, Ala246, Val248, His259, Asn260, His263, Phe264, Met280, Ser282, Val283, Ala286, Cu400, Cu401	11
4c	-9.1021	1.2405	Gly281, Arg268, Glu322	-	His61	His85, His244, Ala246, Val248, His259, Asn260, His263, Phe264, Leu275, Ser282, Val283, Ala286, Cu400, Cu401	12
4d	-8.7425	1.0037	Val247, Arg268	-	His61, His296	His85, Val248, Met257, His259, Asn260, His263, Phe264, Gly281, Ser282, Val283, Phe292, Cu400, Cu401,	11
4e	-8.6611	2.6539	His244, Val283, Glu322	Arg268	His61, His296	His85, Gly245, Ala246, Val248, His259, Asn260, His263, Phe264, Ala286, Phe292, Cu400, Cu401	10
4f	-7.9081	1.3852	Val248, Val283	-	His61	His85, His244, Gly249, Met257, His259, Asn260, His263, Phe264, Ala286, Phe292, Cu400, Cu401	9

Figure 3. Spatial arrangement of compound **4c** with the protein

Based on **Table 2**, it seemed that compound **4a-4f** has the binding free energy lower than the binding free energy of kojic acid. All compounds except tropolone have hydrogen bonding interactions in the active site. Notably, **4c** and **4e** have three hydrogen bonding with Gly281, Arg268, Glu322 and His244, Val283, Glu322, respectively. In opposite, compound **4a** was only able to form hydrogen bonding interaction with Arg268. In addition, compounds **4c** have highest bonding similarity with factor of binding of 12 compared to kojic acid. Factor of binding is the probability for receptor-ligand binding to the same amino acid with the positive control. These probably caused that these compounds become active. Hydrogen bonding and factor of binding may use to predict which compounds will be more active as tyrosinase inhibitor. Furthermore, root mean square deviation is also play an important role for prediction of potentially bioactive compound. Based on the docking results predict that **4c** to be active compound because of some reasons. Firstly, this compound has the lowest binding free energy value of -9.1021 kcal/mol. Secondly, **4c** was constructed three hydrogen bonding through amino acid residues Gly281, Arg268, Glu322 and exhibited van der Waals interaction with His61 inside the binding site of the tyrosinase. Most importantly, **4c** interact with copper atom which have significant role in tyrosinase enzymatic activity. The result suggested that the existence of hydroxyl group in *para* position may enhance the ability to make this molecule bind into the binding pocket with purposing to maintain a high inhibitory activity. The spatial arrangement of **4c** with the protein is depicted in **Figure 3**.

The biological assay proved **4c** is the most active compound as tyrosinase enzyme inhibitor with IC_{50} value of 30.14 μM. Similarly, **4d** and **4e** compounds

are active in both molecular docking study and *in vitro* assay but slightly weaker compared to **4c**. On other hand, despite good binding free energy and binding interaction of 4a, 4b, and 4f in molecular docking, the inhibitory activity of them is very weak in experiment. This indicated that these compounds are active compounds but uncompetitive inhibitor. An uncompetitive inhibitor results inactive enzyme-substrate-inhibitor complex by binding to the enzyme-substrate complex. This is the main reason from docking results shown that these compounds were able to bind well with the protein but the opposite results from the biological assay (Lu et al., 2020)

CONCLUSIONS

In this study, a series of 1,3,5-triphenyl pyrazolines contain sulfonamide, hydroxy, and methoxy group (**4a-f**) have been successfully synthesized via three-component reaction in a sealed-vessel reactor. The chemical structures of all the synthesized compounds were confirmed by spectroscopic analyses and their tyrosinase inhibitory activity were evaluated through molecular docking and in vitro evaluation against tyrosinase enzyme. Compounds **4a**, **4b**, and **4f** have low inhibitory activity with IC_{50} values > 100 μM. On the other hand, compounds **4c**, **4d**, and **4e** surprisingly showed significant inhibitory activity to tyrosinase enzyme, stronger than kojic acid as reference inhibitor. Among all synthesized compounds, **4c** exhibited the lowest IC_{50} value of 30.14 μM. This result revealed that the substituents at *para* position is preferable. The result of in vitro evaluation also agreed with the docking result. Binding mode of **4c** indicated that *p*-sulfonamide and *p*-hydroxyl substituents play important role to provide hydrogen bond interactions with essential amino acid residues in the active site of the enzyme. Thus, it can

be concluded that compound **4c** has a very good potential for further development as a candidate for tyrosinase inhibitor.

ACKNOWLEDGEMENTS

REFERENCES

Ahmad, A., Husain, A., Khan, S. A., Mujeeb, M., & Bhandari, A. (2016). Synthesis, antimicrobial and antitubercular activities of some novel pyrazoline derivatives. *Journal of Saudi Chemical Society*, *20*, 577–584. https://doi.org/https://doi.org/10.1016/j.jscs.2014.12.004

Castro, A., Costa, A. M., & Vilarrasa, J. (2017). The performance of several docking programs at reproducing protein-macrolide-like crystal structures. *Molecules*, *22*(1), 136–150. https://doi.org/https://doi.org/10.3390/molecules22010136

Chang, T.-S. (2009). An updated review of tyrosinase inhibitors. *International Journal of Molecular Sciences*, *10*(6), 2440–2475. https://doi.org/ https://doi.org/ 10.3390/ijms10062440

Cui, H.-X., Duan, F.-F., Jia, S.-S., Cheng, F.-R., & Yuan, K. (2018). Antioxidant and tyrosinase inhibitory activities of seed oils from *Torreya grandis* Fort. ex Lindl. *Biomed Research International*, *2018* (5), 1-10. https://doi.org/https://doi.org/10.1155/2018/5314320

Di Petrillo, A., González-Paramás, A. M., Era, B., Medda, R., Pintus, F., Santos-Buelga, C., & Fais, A. (2016). Tyrosinase inhibition and antioxidant properties of *Asphodelus microcarpus* extracts. *BMC Complementary Medicine and Therapies*, *16*, 453. https://doi.org/https://doi.org/10.1186/s12906-016-1442-0.

Dona, R., Furi, M., Frimayanti, N., Zamri, A., & Nahdiah, N. (2022). Study in silico dan pengaruh gugus metoksi pada hasil sintesis analog kalkon terhadap inhibisi enzim α-glukosidase (In silico study and the effect of methoxy on the results of chalcone analog synthesis as α-glucosidase inhibitor). *Jurnal Sains Farmasi & Klinis*, *9*(1), 12–13.

Farooq, S., & Ngaini, Z. (2020). One pot and two pot synthetic strategies and biological applications of epoxy-chalcones. *Tetrahedron Letters*, *61*, 151416. https://doi.org/https://doi.org/10.1007/s42250-020-00128-5

Hasegawa, T. (2010). Tyrosinase-expressing neuronal cell line as in vitro model of parkinson's disease. *International Journal of Molecular Science*, *11*, 1082–1089. https://doi.org/https://doi.org/10.3390/ijms11031082

Herfindo, N., Prasetiawati, R., Sialagan, D., Frimayanti, N., & Zamri, A. (2020). Synthesis, antiproliferative activity and molecular docking studies of 1,3,5-triaryl pyrazole compound as estrogen α receptor inhibitor targeting MCF-7 cells line. *Molekul*, *15*, 18–25. https://doi.org/https://doi.org/10.20884/1.jm.2020.15.1.585

Jasril, J., Ikhtiarudin, I., Hasti, S., Reza, A. I., & Frimayanti, N. (2019). Microwave-assisted synthesis, in silico studies and in vivo evaluation for the antidiabetic activity of new brominated pyrazoline analogs. *Thai Journal of Pharmaceutical Sciences*, *43*(2), 83–89.

Jusril, N. A., Muhamad Juhari, A. N., Abu Bakar, S. I., Md Saad, W. M., & Adenan, M. I. (2020). Combining in silico and in vitro studies to evaluate the acetylcholinesterase inhibitory profile of different accessions and the biomarker triterpenes of *Centella asiatica*. *Molecules*, *25*(15), 3353. https://doi.org/https://doi.org/10.3390/molecules25153353

Loizzo, M. R., Tundis, R., & Menichini, F. (2012). Natural and synthetic tyrosinase inhibitors as antibrowning agents: an update. *Comprehensive Reviews in Food Science and Food Safety*, *11*, 378–398. https://doi.org/https://doi.org/10.1111/ j.1541-4337.2012.00191.x

Lolak, N., Boga, M., Tuneg, M., Karakoc, G., Akocak, S. &, & Supuran, C. T. (2020). Sulphonamides incorporating 1,3,5-triazine structural motifs show antioxidant, acetylcholinesterase, butyrylcholinesterase, and tyrosinase inhibitory profile. *Journal of Enzyme Inhibiton and Medicinal Chemistry*, *35*, 424–431. https://doi.org/https://doi.org/ 10.1080/ 14756366.2019.1707196

Lu, H., Qi, Y., Zhao, Y., & Jin, N. (2020). Theoretical studies on the selectivity mechanisms of glycogen synthase kinase 3β (GSK3β) with pyrazine ATP-competitive inhibitors by 3DQSAR, molecular Docking, molecular Dynamics simulation and free energy calculations. *Current Computer-Aided Drug Design*, *16*, 31–44.

Makeneni, S., Thieker, D. F., & Woods, R. J. (2018). Applying pose clustering and MD simulations to eliminate false positives in molecular docking. *Journal of Chemical Information and Modelling*, *58*, 605–614. https://doi.org/https://doi.org/10.1021/acs.jcim.7b00588

Mojzych, M., Dolashki, A., & Voelter, W. (2014). Synthesis of pyrazolo[4,3-e][1,2,4]triazine sulfonamides, novel Sildenafil analogs with tyrosinase inhibitory activity. *Bioorganic Medicinal Chemistry*, *22*, 6616–6624. https://doi.org/https://doi.org/ 10.1016/ j.bmc.2014.10.009.

Mojzych, M., Tarasiuk, P., Kotwica-Mojzych, K., Rafiq, M., Seo, S.-Y., Nicewicz, M., & Fornal, E. (2017). Synthesis of chiral pyrazolo[4,3-e][1,2,4]triazine sulfonamides with tyrosinase and urease inhibitory activity. *Journal of Enzyme Inhibition and Medicinal Chemistry*, *32*, 99–105. https://doi.org/https://doi.org/10.1080/14756366.2016.1238362.

Pillaiyar, T., Manickam, M., & Namasivayam, V. (2017). Skin whitening agents: medicinal chemistry perspective of tyrosinase inhibitors. *Journal of Enzyme Inhibition and Medicinal Chemistry*, *32*, 403–425. https://doi.org/https://doi.org/10.1080/ 14756366.2016. 1256882

Pollock, S., Taylor, S., Oyerinde, O., Nurmohamed, S., Dlova, N., Sarkar, R., Galadari, H., Manela-Azulay, M., Chung, H. S., Handog, E., & Kourosh, A. S. (2020). The dark side of skin lightening: An international collaboration and review of a public health issue affecting dermatology. *International Journal of Women's Dermatology*, *7*, 158–164. https://doi.org/https://doi.org/10.1016/j.ijwd.2020.09.006

Qin, H.-L., Shang, Z.-P., Jantan, I., Tan, O. U., Hussain, M. A., Sher, M., & Bukhari, S. N. A. (2015). Molecular docking studies and biological evaluation of chalcone based pyrazolines as tyrosinase inhibitors and potential anticancer agents. *RSC Advances*, *5*, 46330–46338. https://doi.org/https://doi.org/10.1039/C5RA02995C

Rahayu, R., Herfindo, N., Ocsifiani, N., Frimayanti, N., & Zamri, A. (2022). Synthesis of 4-(5-(2, 3-dimenthoxyphenyl)-3-(4-methoxyphenyl)-4, 5-dihydro-1H-pyrazol-1-y1) benzenesulfonamide as a promosing tyrosinase inhibitor candidate. *Jurnal Riset Kimia*, *13*, 49–57. https://doi.org/https://doi.org/10.25077/jrk.v13i1.486

Yusuf, D., Davis, A. M., Kleywegt, G. J., & Schmitt, S. (2008). An alternative method for the evaluation of docking performance: RSR vs RMSD. *Journal of Chemical Information and Modelling*, *48*, 1411–1422. https://doi.org/https://doi.org/10.1021/ci800084x

Zamri, A., Teruna, H. Y., & Ikhtiarudin, I. (2016). The influences of power variations on selectivity of synthesis reaction of 2'-hydroxychalcone analogue under microwave irradiation. *Molekul*, *11*(2), 299–307.

Zamri, A., Teruna, H. Y., Wulansari, S., Herfindo, N., Frimayanti, N., & Ikhtiarudin, I. (2019). 3-(3,4-Dimethoxyphenyl)-5- (2-fluorophenyl)-1-phenyl-4,5-dihydro-1H-pyrazole. *Molbank*, *2019*(4), 1088. https://doi.org/https://doi.org/10.3390/M1088